Gaussian fitting in gamma-ray spectral decomposition

FU Chen WANG Nanping*

Key Laboratory of Geo-detection (China University of Geosciences, Beijing), Ministry of Education, Beijing 100083, China

Abstract In order to extract the information of 662-keV ^{137}Cs spectra from the overlapping peaks with 583-keV ^{208}Tl, 609-keV ^{214}Bi, the overlapping peaks are measured by in-situ γ-ray spectrometer using a NaI(Tl) detector. The spectral model is optimized by the Gaussian fitting algorithm, and the optimized fitting indexes for fitting/original value are from 0.96 to 0.99. Gaussian fitting verified by experiment is feasible for γ-ray spectrum analysis. The full energy peak of ^{137}Cs is extracted correctly from the overlapping peaks, it is important for in-situ γ-ray spectrometer to estimate contamination of ^{137}Cs in radiated environment and nuclear accident.

Key words Gamma-ray spectrum, Gaussian fitting, Overlapping peaks, Decomposition and fitting

1 Introduction

The ^{137}Cs is an important radionuclide for monitoring a nuclear accidents in a nuclear power plant (NPP)[1]. And airborne γ-ray spectrometry has been used for environmental radioactive monitoring since 1980s. Also, in-situ γ-ray spectrometry is used to determine natural radioactivity of uranium, thorium and potassium in rocks or soil, for geological mapping and environmental assessment[2].

A NaI(Tl) detector is of high efficiency and convenience for γ-ray measurement, but it is limited by the low energy resolution and high Compton scattering background. For geological applications, where ^{214}Bi (609 keV) and ^{208}Tl (583 keV) coexist with ^{137}Cs (662 keV), the three γ-ray peaks overlap and this results in large calculation error of the ^{137}Cs activity[3]. Therefore, a fitting algorithm is important for obtaining an accurate activity of the ^{137}Cs. The full peaks in γ-ray spectrometry can be extracted by Monte Carlo simulation and filtering techniques[4,5]. In this study, γ-ray spectra were decomposed by Gaussian fitting algorithm using the least squares approximation. The simulated spectra were compared with measured spectra. The ^{137}Cs activity is extracted correctly.

2 Principle of Gaussian fitting

The energy spectra of a nuclide measured by γ-ray spectrometry are generally in accord with the principle of statistical fluctuation, and Gaussian distribution), as described by Eq.(1),

$$G(x_j)=\sum_i G_i(x_j)=\sum_i A_i \exp[-4(\ln 2)(\frac{x_j-p_i}{B_i})^2] \quad (1)$$

where A_i, B_i and p_i are parameters to determine a characteristic γ-ray peak, i.e. the peak height, FWHM and center of the i^{th} peak, respectively[6].

The Gaussian fitting with the least squares is approximately solved by the MATLAB optimization toolbox providing the 'lsqcurvefit' function[7], and used for large-scale algorithm in subspace trust region based on the interior-reflective Newton method[8].

3 Experimental

All spectra for the Gaussian fitting were recorded with a portable γ-ray spectrometer. It consists of a 3"×3" NaI(Tl) detector, PC-MCA, power supply, spectral stabilizer, display, data storage, and transmission circuit[9]. Its energy resolution is 7.5% at 662 keV.

The γ-ray measurements were performed with a ^{137}Cs source of about 3.7×10^4 Bq, a ^{238}U source (412

Supported by National Natural Science Foundation of China (No. 40274023 and No. 40674067)
* Corresponding author. *E-mail address*: npwang@cugb.edu.cn
Received date: 2009-09-05

Bq) in uranium-radium equilibrium, and a ^{232}Th source (339.7 Bq). The ^{137}Cs, ^{232}Th and ^{238}U γ-ray spectra were collected without lead shield for Gaussian fitting.

And the γ-ray spectra were collected in a lead shield to verify the simulation results. The ^{137}Cs γ-ray counting rate was adjusted by changing the source-to-detector distance from 50 cm to 100 cm, while the ^{238}U and ^{232}Th source were placed in close contact with the detector, because of their low activities. In this setting-up, some of the ^{137}Cs γ-ray was absorbed by the ^{238}U and ^{232}Th sources. When measuring the single spectrum of ^{137}Cs γ-ray, the ^{238}U and ^{232}Th sources were replaced by a ^{40}K source and a cylinder filled with SiO_2 and Al_2O_3. The measured spectra of ^{232}Th, ^{238}U and ^{137}Cs sources were compared with the Gaussian fitting.

The γ-ray measurement conditions in a 5-cm thick lead shield are shown in Table 1.

Table 1 Experimental conditions for measuring ^{137}Cs, ^{232}Th and ^{238}U γ-ray spectra in a lead shield.

Spectra	Radionulides	Source position
701, 702, 703	^{137}Cs, ^{238}U, ^{232}Th	Place the ^{238}U, ^{232}Th and ^{137}Cs sources in front of to the detector, with the ^{238}U and ^{232}Th sources side by side, at 0 cm to the detector, and the^{137}Cs source at 50 cm (701), 70 cm (702) and 100 cm (703).
704	^{232}Th	Remove the ^{137}Cs and ^{238}U sources to measure the single 583-keV peak of ^{232}Th.
705	^{238}U	Remove the ^{137}Cs and ^{232}Th sources to measure the single 609-keV peak of ^{238}U.
706, 707, 708	^{137}Cs	Replace the ^{238}U and ^{232}Th sources with a ^{40}K source and a cylinder of SiO_2 and Al_2O_3, to measure the single 662-keV peak of ^{137}Cs with the source at 50 cm (706), 70 cm (707) and 100 cm (708) to the detector.

Table 2 Parameters of the separated tri-overlapping peaks at the ^{137}Cs source-to-detector distance of 50 and 100 cm.

Parameters	50 cm			100 cm		
Energy / keV	583	609	662	583	609	662
Peak height / cps	0.11	0.16	0.63	0.11	0.18	0.19
FWHM	14.11	13.31	13.47	8.84	11.22	12.45
Net area / cps	1.69	2.32	9.11	1.07	2.13	2.58

4 Gaussian fitting of overlapping peaks

4.1 Results of Gaussian fit

Before fitting, the straight-line background is deducted by processing software of γ-ray spectrum using Eq.(2), such as MAESTRO-32, and Gamma Vision^{TM} -32,

$$B_i = \frac{C_h - C_l}{h-l} \times i + (C_l - \frac{C_h - C_l}{h-l} \times l) \quad (2)$$

where B_i is the background contents of channel i, l and h are the low/high margin of ROI (region of interest), C_l is the average contents of channels(l–1), l and (l +1), and C_h is that of (h–1), h and (h+1). The overlapping peaks at 583, 609 and 662 keV were decomposed and fitted by using the Matlab 6.5 code, and their centers were determined by energy calibration. Table 2 shows parameters of the separated tri-overlapping peaks.

As we changed just the ^{137}Cs source position, the parameters were fixed for the decomposed 583 and 609-keV peaks under identical conditions. Table 2 shows that the ^{137}Cs activity (net areas) at the source-to-detector distance of 100 cm is smaller than that at 50 cm, the FWHM changes a little. However, For other source-detector-distances between 50 cm and 100 cm, the FWHM became significantly narrower (not shown), as the scattering became smaller, and this may affect the decomposition.

The fitting quality was evaluated by the fitting optimization index (R^2)[10],

$$R^2 = 1 - \frac{\sum (y - \hat{y})^2}{\sum (y - \overline{y})^2}. \quad (3)$$

where, R^2 is the correlation coefficient, y is the fitting data, $\hat{y}$ is the original data, and $\overline{y}$ is the average of original data.

Table 3 shows the fitting parameters of tri-overlapping peaks for other γ-ray spectra emitted from the mixed sources.

Table 3 Parameters of the separated tri-overlapping peaks.

Spectra	583-keV Peak		609-keV Peak		662-keV Peak		R^2
	Peak height / cps	FWHM	Peak height / cps	FWHM	Peak height / cps	FWHM	
801	–0.42	14.50	0.66	23.41	12.4	16.90	0.99
802	–0.07	11.17	0.10	17.44	5.02	17.19	0.99
803	0.09	21.38	–0.09	30.12	2.68	17.55	0.99
806	0.05	13.82	0.11	12.77	0.67	17.52	0.99
807	0.01	21.33	0.11	17.64	0.91	17.33	0.99
808	0.03	15.88	0.11	15.88	1.13	17.52	1.00
809	0.01	16.96	0.10	14.87	1.45	17.40	1.00
810	0.03	14.55	0.11	10.44	2.01	17.72	0.99
911	0.03	15.16	0.11	13.34	0.74	18.44	1.00

Table 4 Comparison of the net area ratios of the separated / measured single peaks.

Spectra	Energy / keV	Peak height / cps	FWHM	N1 / cps	N2 / cps	Error of net area / %
703	583	0.08	12.35	0.99	1.21	–18.18
	609	0.21	12.68	2.87	2.66	7.89
	662	0.21	15.95	3.57	3.63	–1.65
	Whole area / cps			7.43	7.5	–0.93
702	583	0.09	12.03	1.21	1.21	0
	609	0.23	12.75	3.08	2.66	15.79
	662	0.41	14.66	6.46	6.44	0.31
	Whole area / cps			10.75	10.31	4.27
701	583	0.11	12.02	1.45	1.21	19.83
	609	0.22	12.9	3.02	2.66	13.53
	662	0.81	14.99	13.00	12.97	0.23
	Whole area / cps			17.47	16.84	3.74

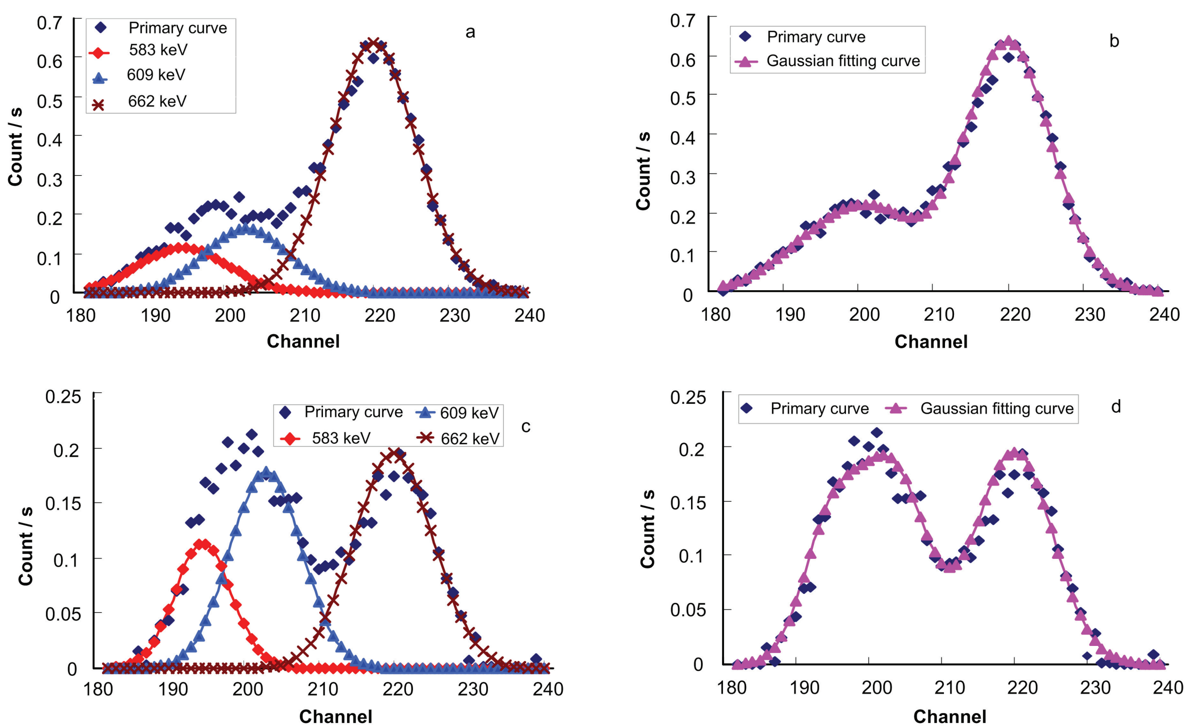

Fig.1 The fitting and decomposed curves for the tri-overlapping peaks at different source-to-detector distances. (a & b, 50 cm; c & d, 100 cm: a & c, primary curve and separated peak with Gaussian fitting; b & d, primary and Gaussian fitting curves).

The optimal fitting indexes were 0.99 to 1.0. The FWHM for 583- and 609-keV peaks varied asymmetrically except for the stable 662-keV peak, and some of the peak heights for 583- and 609-keV peaks were negative. These situations often appear when the net area of 662-keV peak is 10 times larger than that of 583- and 609-keV peaks.

4.2 Verification of Gaussian fitting

Fig.1 shows that overlapping peaks were decomposed and fitted by Gaussian fitting. The closer to 1 the R^2 was, the better the fitting curve. The optimal indexes for fitting and original curve were 0.99 and 0.96. In order to validate reliability of the peak-decomposing, the spectrum of a signal source was measured and compared with separated peak from fitting. In Table 4, the N1 and N2 were the net areas of the separated and measured single peaks, respectively. The 662-keV peak of spectrum 703, 702 and 701 had errors of –1.65, 0.31, and 0.23%, respectively. And net areas of the 583- and 609-keV peaks had larger errors due to the overlapped ROI regions. This shows that the ^{137}Cs activity is extracted accurately by Gaussian fitting.

5 Conclusions

The overlapping peaks for 583, 609 and 662 keV are decomposed by Gaussian fitting. The ^{137}Cs activity is extracted correctly at the inflexions of 662 and 609 keV. The ROI ranges of 583- and 609-keV peaks overlap almost together, and net areas are smaller than of ^{137}Cs. The poor and negative peak areas need be further fitted.

References

1 Wang H D. Radiat Prot Bull, 2000, **20:** 38–41.

2 Cheng Y X, Wang N P, Hou S L. Nucl Geophys Surv, Beijing: Geological Publishing House, 2005, 97–280.

3 Dubois G, Cort M D. J Environ Radioact, 2001, **53:** 271–289.

4 Allyson J D, Sanderson D C W. J Environ Radioact, 1998, **38:** 259–282.

5 Guillot L. J Environ Radioact, 2001, **53:** 281–398.

6 Pei S Y. Master's thesis. Beijing: The school of geophysics and information technique, China University of Geosciences (Beijing), 2005, 6–20.

7 Xue D Y. Advanced applied mathematical problem solution with MATLAB. Beijing: Tsinghua University Press, 2004, 210–226.

8 F T, Li Y. Math Prog, 1994, **67:** 189–224.

9 Wang N P, Pei S Y, Huang Y. Radiat Prot, 2005, **25:** 347–356.

10 Ni Z C. Medical Statistics. Beijing: People's Medical Publishing House, 1990, 143–148.